When are actively balanced biphasic ('Lilly') stimulating pulses necessary in a neurological prosthesis? I Historical background; Pt resting potential; *Q* studies

N. de N. Donaldson P. E. K. Donaldson

MRC Neurological Prostheses Unit, 1 Windsor Walk, London SE5 8BB, England

Abstract—*Actively balanced ('Lilly') stimulating current waveforms are generally considered to give very 'safe' stimulation. Although this is perfectly true, the specification of the necessary waveform generators in neurological prostheses demands additional complexity, and probably additional expense and development time as well. The paper and its companion enquire whether the use of simple, passively charge-balanced stimulating pulses is equally safe, provided the stimulation parameters and circuitry are designed with appropriate care. It is concluded that, in respect of safe deliverable charge density per pulse at the electrode, release of noxious products and stimulating effectiveness, simple pulses need give no worse performance; in some circumstances they may give better.*

Keywords—*Electrochemistry, Electrodes, Platinum, Stimulation*

Med. & Biol. Eng. & Comput. 1986, **24**, 41-49

1 Introduction

In 1952, Lilly, Austin and Chambers (Lilly *et al.*, 1952) reported some investigations into the effects of varying stimulus parameters on the threshold for cerebral cortical stimulation in cats and monkeys. Unidirectional current pulses were led to and from the preparation via large reversible electrodes and saline-filled capillaries. Separating the electrodes from the tissue in this way removed many of the mechanisms by which 'direct' electrode stimulation might cause tissue damage: pH changes, gas evolution, bleach production, $Mg(OH)_2$ deposition, electrode metal dissolution etc.; the stimulating current produced negligible I^2R heating. However, tissue damage was still observed, which the authors suggested was proportional in severity to the total net transfer of charge during the stimulation period.

Three years later, the celebrated letter appeared in *Science*, from Lilly, Hughes, Alvard and Galkin, reporting that brain damage was undetectable if brief (34 μs) stimulating current pulses were followed 100 μs later by a similar current pulse in the opposite direction (Lilly *et al.*, 1955). They claimed that the stimulating arrangement they used balanced the charges moved by the two pulses to within 0·4 per cent. They evidently felt that what was important was not that they had achieved almost zero net charge transfer but that they had achieved it from two pulses of similar amplitude and duration, for they wrote 'Other similarly balanced *brief* (our italics) waveforms would probably give similar results'.

First received 29th October 1984 and in final form 19th February 1985

There are of course other ways of ensuring no, or almost no, net transfer of charge. Using a unidirectional current-pulse generator whose output resistance is not too high, one may merely connect a capacitor in series with the electrodes. Or, if the electrodes are polarisable (e.g. platinum), one may utilise the electrode capacitance itself to achieve charge balance by allowing the electrode capacitance to discharge back through the output resistance of the stimulator between pulses ('exhausting the electrode'). These 'passive' balancing schemes also cause biphasic currents to flow, but the two phases may not be at all similar (Fig. 1). The great question is, how much does the dissimilarity matter? Lacking complete understanding of the electrode, its charge-injection processes and their neuropathological effects, it is commendably cautious to argue that, if electrochemical species are to be released into extracellular fluid during the stimulating phase, one had better use a 'Lilly' wave, or something like it, to recover those species before they diffuse away and are lost (e.g. Berkley, 1965). Perhaps as a result of such caution, the platinum electrode injecting double (opposite) pulses has received a good deal of attention, notably from S. B. Brummer and his co-workers. Using platinum and a variety of more-or-less physiological electrolytes, they have studied *in vitro* the safe injectible charge (Brummer and Turner, 1977*b*; *c*), the oxidation of chloride (Brummer *et al.*, 1977) and loss of metal from the electrode (McHardy *et al.*, 1980; Robblee *et al.*, 1980). More recently they have looked at the performance of iridium electrodes, with promising results (Robblee *et al.*, 1983).

The neurological prosthesis designer, however, is pressed for space. His implantable stimulators need to be rugged and simple, able to continue working in the face of drifts in

component values, perhaps even fault conditions. He would prefer not to be asked to make double-pulse current generators whose pulse-pairs are matched to better than 1 per cent if he can achieve satisfactory results by making a simple pulse and using passive charge balancing. Though willing to make an active charge balanced auditory prosthesis having three or four output channels (e.g. British Patent Application No. 8301526) he would be loath to extend the technique to a visual prosthesis having several hundred output channels.

It seemed to us, therefore, that we should look again at the behaviour of platinum electrodes fed with single-pulse waveforms, with particular reference to those performance indices studied by Brummer and his group. In doing so, we made some incidental observations which we thought interesting and worth including in the paper.

2 The problem of safe injectible charge

The amount of charge which a platinum or platinum-alloy electrode can inject, per pulse, is limited by the capacitative nature of the electrode/electrolyte interface, and its breakdown voltage. Continued passage of current from electrode to electrolyte, or vice versa, raises or depresses the potential difference across the interface until a critical value is reached and the capacitor-like behaviour breaks down. Thereafter, current-carrying is mediated by substantially irreversible electrochemical processes which are harmful to tissue.

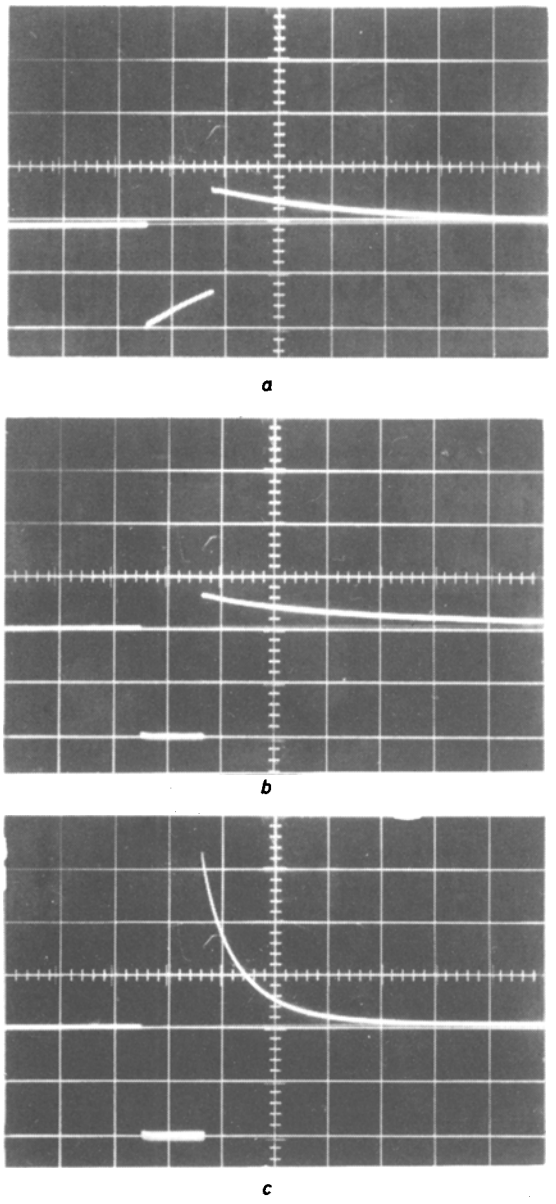

Fig. 1 *Passive balanced stimulating current waveforms; (a) using series capacitor and pulse generator having constant output resistance, (b) directly coupled, but output resistance switched to achieve satisfactory exhaustion, (c) using series capacitor and switching of output resistance to obtain very rapid exhaustion*

If ϕ is the potential of the electrode with respect to a reference electrode in the same electrolyte, ϕ_{max} is the most positive allowable value of ϕ, ϕ_{min} is the most negative allowable value, C_e is the pseudocapacitance of the interface (a nonlinear function of ϕ), ϕ_1 is the value of ϕ just before the beginning of a pulse and Q is the injectible charge, then

$$Q_{a\,max} = \int_{\phi_1}^{\phi_{max}} C_e \, d\phi \quad \text{for a stimulating anode,}$$

and

$$Q_{c\,max} = -\int_{\phi_{min}}^{\phi_1} C_e \, d\phi \quad \text{for a stimulating cathode.}$$

The problem is solved when we know ϕ_{max}, ϕ_{min}, ϕ_1 and C_e. A further important quantity is ϕ_0, the value of ϕ for an electrode passing no current, merely left to come into equilibrium with its surrounding. $\phi_1 \approx \phi_0$ at the beginning of a train of stimulating pulses if the electrodes have previously been quiescent for some minutes. Thereafter, ϕ_1 may shift to a new value.

2.1 *The resting potential of a platinum electrode, ϕ_0*

A platinum electrode, whether in saline or implanted in extracellular fluid, behaves quite differently from a reversible electrode such as the Ag/AgCl. Whereas the latter, in chloride-containing solution, exhibits a definite potential, in accordance with its position in the electrochemical series and a low resistance, the former can be set at some potential between ϕ_{max} and ϕ_{min} and over periods typical of the duration of stimulation waveforms it will remain there. While the reversible electrode is reminiscent of a low resistance in series with a source of EMF, the platinum electrode behaves more like a capacitor with rather low breakdown voltage.

But it is a leaky capacitor. Over the course of minutes, the potential of a platinum electrode previously charged to some arbitrary value will be found to drift to a new, equilibrium value determined by conditions in the electrolyte. *In vitro*, the nature and amount of dissolved gas, the pH and the amount of protein, if present, all affect the resting potential. A piece of platinum in unbuffered Tyrode's solution in equilibrium with South London air in this laboratory at room temperature settled to +600 mV NHE.* Bubbling in 95 per cent O_2, 5 per cent CO_2 raised the potential to +665 mV. Purging the electrolyte of oxygen by bubbling in argon reduced the resting potential to +425 mV. Bubbling in hydrogen reduced the potential further, to −250 mV. In another experiment with electrolyte in equilibrium with air, acidifying to pH 1 raised the electrode potential to +630 mV; increasing pH to 11 reduced the potential to +90 mV. The pH dependency was therefore not far from 59 mV pH^{-1}. At pH 7 in serum, the potential was +350 mV, about right if voltage is to be proportional to pH. We do not know if the fall from 600 mV to 350 mV in neutral solution results from a

** All electrode potentials in this paper are quoted against normal hydrogen electrode (NHE), i.e. a platinum electrode bubbled with hydrogen at pH 0. The saturated calomel electrode we actually used sits at +242 mV NHE.*

blocking of the platinum dissolution mechanism by serum protein (ROBBLEE *et al.*, 1980) or from the oxidation of some serum component at the electrode surface. If the former is the case, the results are comprehensible if the electrode is regarded as a short-circuited hydrogen/oxygen fuel cell (Appendix). If the latter, the apparent proportionality between potential and pH is probably fortuitous. For a discussion of ϕ_0 assuming the platinum electrochemically active, see for example HOARE (1967).

We measured the potentials of a platinum and of an 80 per cent Pt, 20 per cent Ir electrode, which had been placed subcutaneously in a rhesus monkey, 3, 7, and 12 weeks after implantation. With a calomel reference poked through the incision, readings averaged +135 mV for the pure Pt electrode and +219 mV for the alloy. Readings were consistently 31 mV more positive if the reference electrode was placed on the animal's tongue.

2.2 *Scanning voltammetry: the ϕQ diagram*

An apparatus such as that outlined in Fig. 2 is helpful in visualising the dynamic performance of a platinum electrode, and in giving meaning to ϕ_{max}, ϕ_{min}, C_e and ϕ_1. A microprocessor is used as a universal pulse generator to switch on and off a power FET. The output is a train of square waves, variable up to 60 V, which is converted to a train of square waves of current by the high resistance R. A large series capacitor C blocks the passage of direct current. The current, whose average value after the first few cycles is zero, is introduced to the electrolyte by a platinum counterelectrode E_c. Thence it enters the platinum electrode under test, E_t, and passes to earth via the integrating capacitor C_i. The voltage across C_i is proportional to the electrode charge Q. ϕ is measured by a differential amplifier reading between E_t and a reference electrode E_r. As this amplifier actually measures ϕ plus a square wave of IR drop caused by the access resistance to E_t, it is convenient to compensate for this drop by feeding into the amplifying chain an appropriate current, controlled by R_c.

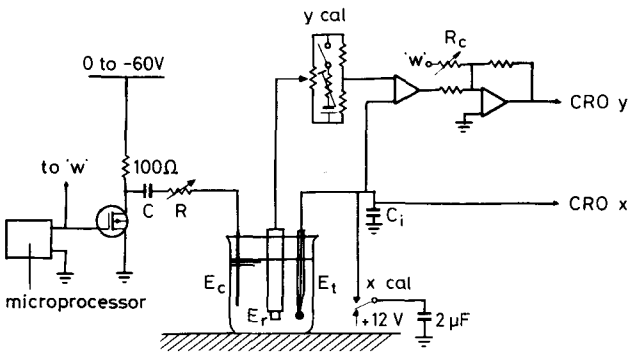

Fig. 2 *Outline of laboratory apparatus to study ϕQ diagrams for capacitor-coupled electrodes. The X cal. switch makes 24 μC pips*

Using an electroetched spherical electrode of geometric surface area 2 mm^2, mounted at the tip of a glass micropipette, for E_t, unbuffered Tyrode's solution, a 1 Hz square wave with unity mark-space ratio, a 60 V power supply, adjusting R until E_t is seen to be just gassing, and with R_c set appropriately, one obtains a ϕQ diagram like Fig. 3*a*. The diagram is not very frequency dependent; Fig. 3*b* shows the corresponding diagram for 16 Hz. Most of the features in Fig. 3*a* are present in Fig. 3*b*, but the latter is somewhat taller because the current is now 16 times greater, necessitating larger overpotentials on the H_2 and O_2 evolution reactions.

The height of the diagram in Fig. 3*a* is about 2 V, which at once tells us something about the pH at the surface of E_t; for the H_2 and O_2 decomposition potentials, corresponding to the flattened regions at the bottom and at the top of the diagram, are well known to be

	pH 0	pH 7	pH 14	
H_2	0	−410	−830	mV NHE
O_2	+1230	+820	+400	

A 2 V swing implies a cyclic local pH variation from nearly 0 at O_2 evolution to 14 at H_2 evolution. The height of the diagram is not affected by the addition of buffer to the electrolyte.

For many stimulation purposes (but see section 5 of the accompanying paper, DONALDSON and DONALDSON, 1986) the oxygen and hydrogen evolution potentials constitute ϕ_{max} and ϕ_{min}. We are now in a position to consider how the platinum electrode injects charge, i.e. what electrochemical processes are available in the range $-830\,\text{mV} < \phi < +1230\,\text{mV}$ NHE.

2.3 *The platinum charge-injection mechanism*

The principal cations in extracellular fluid are Na^{2+}, K^+, Mg^{2+}, Ca^{2+}, all of which reduce at potentials considerably below −830 mV. The principle anions are Cl^- and HCO_3^-. Cl^- oxidises to Cl_2 (chlorine gas), ClO^- (hypochlorite), ClO_2^- (chlorite), ClO_3^- (chlorate), or ClO_4^- (perchlorate) at potentials above +1230 mV (LOEB *et al.*, 1982). HCO_3^- can be regarded as a pairing of a CO_2 molecule with a hydroxyl ion; there is no specific oxidation

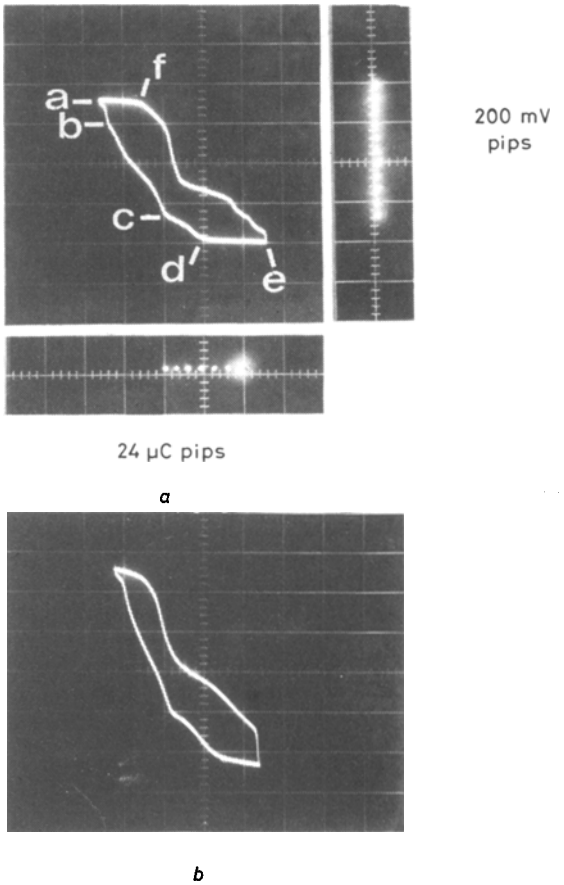

Fig. 3 *(a) Gassing-to-gassing ϕQ diagram for 1 Hz. Positive charge is plotted to the left. The CRO spot runs round the diagram anticlockwise. Horizontal sensitivity: 72 μC division^{-1}, vertical sensitivity: 600 mV division^{-1}, (b) The same, for 16 Hz*

potential for the bicarbonate ion.

Although it is thermodynamically possible for platinum metal to form Pt^{2+} at 1200 mV, in fact platinum group metals do not form simple ions in aqueous solution. They do, however, form complex ions, and as there is chloride available

$$Pt + 4Cl^- \rightleftharpoons PtCl_4^= + 2e$$

$$Pt + 6Cl^- \rightleftharpoons PtCl_6^= + 4e$$

These reactions have equilibrium potentials at 730 and +720 mV, respectively (PETERS and LINGANE, 1962).

Fortunately, most of the charge is injected by redox and hydrogen plating and stripping reactions which are bound to the surface of the metal, e.g.

$$Pt + 2H_2O \rightleftharpoons Pt(OH_2) + 2H^+ + 2e \quad (+980\,mV)$$

$$Pt + H_2O \rightleftharpoons PtO + 2H^+ + 2e \quad (+570\,mV)$$

$$Pt + Cl^- + OH^- \rightleftharpoons Pt(OH)Cl + 2e \quad (+400\,mV)$$

$$Pt + H^+ \rightleftharpoons Pt - H - e$$

(see, for example, PETERS and LINGANE, 1962, *loc. cit.*) in some proportion depending on the potential range over which the electrode is worked. Some of these mechanisms have been recognised by electrochemists for nearly 60 years (e.g. BOWDEN, 1929) but were not widely appreciated by electrophysiologists and bioengineers until much later. Many of us thought that noble electrodes injected charge through the double-layer capacitance, that relatively small capacitance, dependent on frequency, which can be measured using small signals from AC bridges (DE BOER and VAN OOSTEROM, 1978; ONARAL and SCHWAN, 1982) and which is relevant when *recording* biopotentials. WEINMAN and MAHLER warned against this idea in 1964, when they wrote 'Electrical constants of metal electrode thus ..... (i.e. by bridge methods) ..... obtained do not, however, describe the behaviour of metal electrodes in electrophysiological experiments'. As recently as 1973, GREATBATCH wrote 'our studies have now convinced us that electricity couples into the body through platinum electrodes by a modulation of the level of catalytically absorbed oxygen on the surface of each electrode.' It was Brummer and Turner who drew engineers' attention to the hydrogen-plating reaction, complementing the redox reactions, in a paper written in 1974 but not published until three years later (BRUMMER and TURNER, 1977*a*).

Looking at Fig. 3*a* and starting at point *a*, the electrode is covered with a passivating layer, probably a mixture of oxychlorides of Pt^{2+} and Pt^{4+} (PETERS and LINGANE, 1962), and has just been evolving O_2. The segment from *a* to *b* marks the collapse of the oxygen overvoltage; *b* to *c* represents the progressive reduction of the passivating layer. The prominent feature at *c*, 'Brummer's point' (BRUMMER and TURNER, 1977*b*) is a ubiquitous milepost in ϕQ studies which marks the completion of surface reduction and the beginning of hydrogen plating. It occurs at approximately −400 mV NHE. At *d* the plating process is complete and the electrode begins to evolve H_2. $\phi = \phi_{min}$. According to Brummer and Turner, the horizontal width of the segment *c–d* is a measure of the real surface area of the electrode; they assert it takes 232 μC to hydrogen-plate 1 real cm^2. This particular electrode took 72 μC to plate it, and so the area was really 31 mm^2; a roughening factor of about 15.

In moving from *a* to *d* the electrode injected reversibly a total of −180 μC; from *d* to *e* it injected −180 μC irreversibly, evolving H_2. In passing from *e* to *f*, stripping off the hydrogen and reoxidising the surface, it injected +216 μC reversibly, then from *f* to *a* a further +72 μC irreversibly, evolving oxygen, ready for a new cycle.

Between *b* and *c*, $dQ = -108\,\mu C$ and $d\phi = -1400$ mV, so the 'oxide' pseudocapitance C_{eO} is 77 μF or 248 μF real cm^{-2}. Between *c* and *d* $dQ = -72\,\mu C$ and $d\phi = -300$ mV, so the 'hydride' pseudocapacitance C_{eH} is 240 μF, or 774 μF real cm^{-2}. On the return trip, fluctuations in slope are so enormous that similar calculations are not useful; fortunately, using the electrode in nongassing modes, C_e is more nearly constant.

2.4 *The capacitor-coupled pulsing cathode*

When a capacitor-coupled platinum electrode is used to inject negative-going stimulating pulses (Figs. 2 and 4) ϕ_1 initially equals ϕ_0 and the potential range available in delivering the first pulse is $(\phi_0 - \phi_{min})$. If the charge per pulse which produces this potential change is exceeded and ϕ taken below ϕ_{min}, the electrode will evolve a little hydrogen at the peak of each negative excursion. The net transfer of charge corresponding to this hydrogen will alter the mean voltage across the series capacitor in such a direction as to bias the electrode positively. ϕ_1 'slides back' from ϕ_0 to some more positive value ϕ_s. Hydrogen evolution now ceases, and the electrode works over the new, greater potential range $(\phi_s - \phi_{min})$. If one continues to raise the charge per pulse, ϕ_s eventually reaches ϕ_{max}, no further 'slide back' is possible, and the electrode begins to evolve both oxygen and hydrogen, alternately, as is happening in Fig. 3. BRUMMER and TURNER (1977*c*) have drawn attention to this mechanism, pointing to the important conclusion that a capacitor-coupled electrode that is evolving hydrogen steadily must also be evolving oxygen; and vice versa.

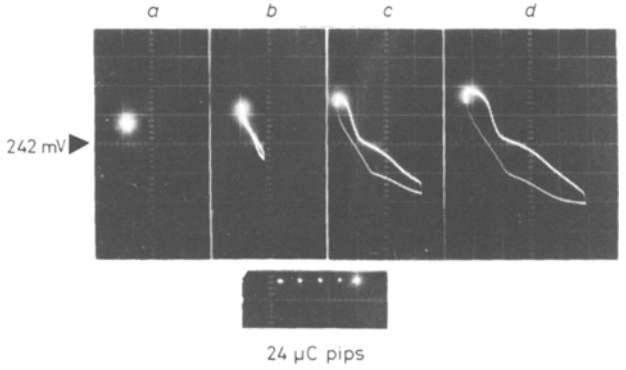

Fig. 4 *Family of ϕQ diagrams for capacitor-coupled cathode. These are 'steady-state' diagrams, each for a different charge per pulse. The 30 ms pulse causes the spot to start downward and to the right. During the 600 ms interval it returns slowly to its point of departure. Horizontal sensitivity: 36 μC division^{-1}, vertical sensitivity: 600 mV/ division^{-1}*

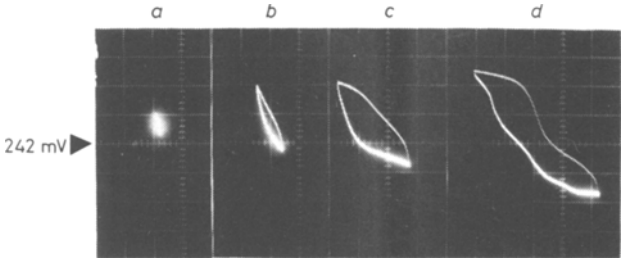

Fig. 5 *Family of ϕQ diagrams for capacitor-coupled anode, complementary to Fig. 4. Horizontal sensitivity: 36 μC division^{-1}, vertical sensitivity: 600 mV division^{-1}*

However, it is not necessary to pulse ϕ below ϕ_{min}, for 'slide-back' to occur. A simple explanation can be seen from the simplified circuit model shown in Fig. 6*a*. The pulse generator feeds the electrode through the series capacitor C and access resistance R_a. C_e and R_e are the electrode pseudocapacitance and leakage resistance, respectively. The impedance of the relatively large counter or indifferent electrode is assumed small and is omitted. The branch containing the diode, the Zener diode and R_{H_2} carries the hydrogen-evolving current. It is clear that, even if $i(t)$ is insufficient to drive any 'hydrogen' current, the network C, R_a, C_e, R_e forms a bandpass filter and the average value of ϕ must be ϕ_0. Hence, if ϕ reaches a value $<\phi_0$ during the pulse, it must return to a 'home value' $>\phi_0$ between pulses. Fig. 4 shows, for 30 ms pulses every 600 ms, the development of cathode slideback as the charge per pulse in Tyrode's solution is gradually increased. ϕ_1 is seen to increase some 600 mV over the range of injected charge used. Only at Fig. 4*d* does gassing occur.

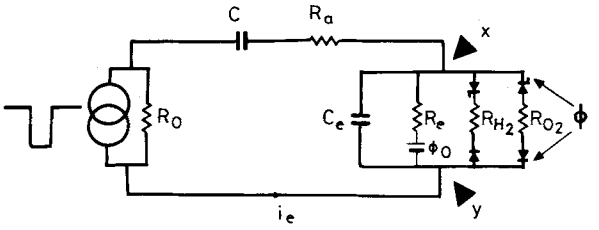

a

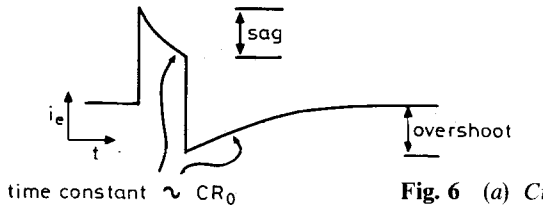

b

Fig. 6 *(a) Circuit model for pulsed capacitor-coupled cathode, (b) effect of finite C and R_0 on current waveform*

Fig. 4 also shows that, for moderate injected charge which does not reach Brummer's point, the electrode behaves as a capacitor fairly constant in value (see the slope in Fig. 4*b*) and also energy efficient, in that the loop encloses a small area. This electrode had a real area of 31 mm^2 and for moderate charge a capacitance of 36 μF. The maximum injectible charge *in vitro* which evolves no hydrogen, even transitorily, is therefore $Q_{c\,max} = -C_{eO}(\phi_0 - \phi_{min}) = -36\ \mu\text{F}(600\text{ mV} + 800\text{ mV}) = -50\ \mu\text{C}$ or $-161\ \mu\text{C}$ real cm^{-2}. The maximum charge if possible transitory evolution of hydrogen is tolerable is best read from Fig. 4*d*, and is approximately $-126\ \mu$C, or $-406\ \mu$C real cm^{-2}.

2.5 *The capacitor-coupled pulsing anode*

By a similar argument to that for the capacitor-coupled cathode, the electrode can operate over a voltage range $(\phi_{max} - \phi_0)$ if no transitory evolution of oxygen can be tolerated, or over a greater range $(\phi_{max} - \phi_s)$ if some liberation is allowable. Here, of course, ϕ_1 slides back from ϕ_0 to some *lower* value ϕ_s. Slideback in a pulsing anode, again for a 30 ms pulse every 600 ms, is shown in Fig. 5. ϕ_1 can be seen moving about 1400 mV negative between 5*a* and 5*d*. Again, the electrode capacitance for moderate charge per pulse is 36 μF (Fig. 5*b*), so that the unconditionally safe charge *in vitro* is $Q_{a\,max} = +C_{eO}(\phi_{max} - \phi_0) = +36\ \mu\text{F}(1230\text{ mV} - 600\text{ mV}) = 28\ \mu\text{C}$ or $90\ \mu$C real cm^{-2}. If temporary oxygen evolution is acceptable, the maximum injectible charge is again about 126 μC or 406 μC real cm^{-2} (Fig. 5*d*).

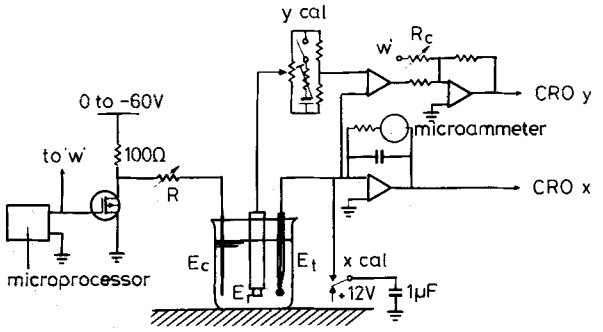

Fig. 7 *Modified arrangement for studying a direct-coupled anode with poor exhaustion. The X cal. switch now makes 12 μC pips*

2.5.1 *Time constant of slideback effect.* It is worth noticing that the time constant for the decay of slideback effects is quite different from the time constant which describes, for example, the 'sag' in the stimulating current pulse (Fig. 6*b*). The latter is given by

$$\left(\frac{CC_e}{C + C_e}\right)(R_0 + R_a)$$

and with practical circuit values will probably approximate CR_0. With $C = 1\ \mu$F and $R_0 = 5\ \text{k}\Omega$, the time constant for pulse sag will be 5 ms. The time constant for slideback decay is the time constant seen looking in between X and Y, and is approxiamtely the product of the pseudocapacitance C_e and the leakage resistance R_e. As seen in Section 2.1, this product may extend to several minutes. The practical importance is that, where stimuli are delivered in bursts, the electrodes remain 'slid-back' between bursts; momentary gassing is not required at the beginning of each burst to re-establish the 'slid-back' condition.

2.5.2 *Choice of series capacitor.* C should be large enough to pass the stimulating pulse without excessive sag, both because sag represents a wasteful loss of charge and because the large overshoot which accompanies severe sag can reduce the efficacy of such stimulating charge as has been delivered (Figs. 6*b* and 1*a*). On the other hand, C must be small enough for the time constant CR_0 to be several times less than the interval between pulses, otherwise the electrode will begin to fill with charge from the second pulse before it has finished emptying from the first. At high stimulus frequencies it may become impossible to satisfy both criteria; a way out of this difficulty is to use a pulse generator whose R_0 is high during the pulse but low between pulses (DONALDSON and DONALDSON, 1986).

2.6 *The direct-coupled pulsing anode*

The ϕQ apparatus is modified as shown in Fig. 7. The series capacitor disappears and a more advanced, feedback, integrator becomes necessary, which holds E_t at earth potentials; this simulates the real-life situation, in which (between pulses) active and passive electrodes are connected together through R_0. The extra operational

amplifier also supplies the voltage required to operate the microammeter used to measure the net electrode current.

Using 20 ms pulses with 60 ms intervals, R set to 30 kΩ, and the variable power supply to control the charge per pulse, one finds that, when the electrode is pulsed, ϕ_1 'slides forward' from ϕ_0 to a more positive value (Fig. 8, *a–g*) which is not far below ϕ_{max}, severely limiting the voltage range available for safe charge injection. The rise is a consequence of an elementary circuit property (Fig. 9*a*). Here the impedance of the counter (passive) electrode/electrolyte junction is again neglected, but the resting potential ϕ_i is important and must be included.

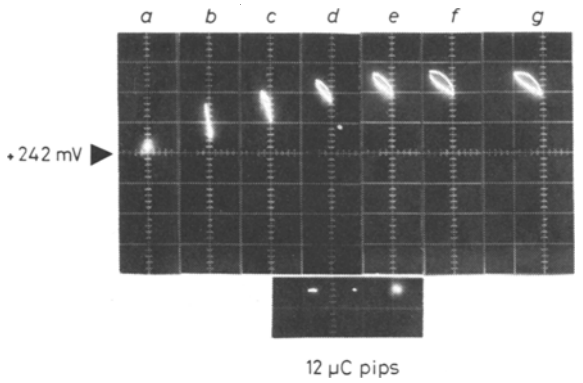

Fig. 8 *Family of ϕQ diagrams for a poorly exhausted direct-coupled anode. 20 ms pulse, 60 ms. Horizontal sensitivity: 9 μC division^{-1}, vertical sensitivity: 600 mV division^{-1}*

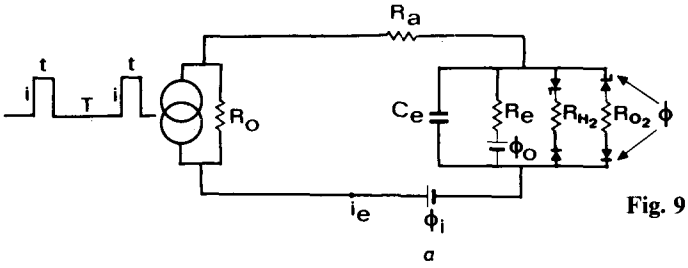

Fig. 9 *(a) Circuit model for poorly exhausted direct-coupled anode, (b) simple RF-coupled stimulator circuit which can be made very small but which offers only poor exhaustion. At very low stimulation frequencies a germanium diode can be used and the resistor omitted*

If the pulse is on for t and off for T, the mean voltage across C_e, ϕ_m, will rise by $iR_0\ t/(t + T)$. Unless $t \ll T$, ϕ_m may be very close to ϕ_{max}, in which case ϕ_1 must be quite close to ϕ_{max} also. This is the plight of the simple RF-coupled stimulator such as that depicted in Fig. 9*b*. Fig. 8*c* shows that, for $t/T = 1/3$, admittedly a very unfavourable ratio for charge recovery, this electrode (which also produced Figs. 3*a* and 4*d*) cannot safely inject more than about $3\frac{1}{2}$ μC per pulse (area = 10 mm^2 real, so 35 μC real cm^{-2} pulse).

2.6.1 *The direct-coupled pulsing anode, with exhaustion.* By rearranging the ϕQ apparatus as shown in Fig. 10, the electrode charging current remains the same, but the discharging current is much increased, limited mainly by the access resistance, which, for a 0·8 mm diameter ball in extracellular fluid or Tyrode's solution, is about 100 Ω. Altering the generator so that the output resistance is lowered between pulses yields 'exhaustion' of the electrode. ϕQ diagrams, again for $t/T = 1/3$ for a well exhausted direct-coupled anode, are shown in Fig. 11, *a–f*. ϕ_1 remains at ϕ_0, maintaining the difference between ϕ_1 and ϕ_{max} so that a satisfactory charge can be safely injected. (In fact, ϕ_1 actually *falls* slightly. We believe this to be a slideback resulting from the unavoidable series capacitance provided by E_C.) The situation depicted in Fig. 11*f* is probably safe; the anode is seen to be injecting 9 μC per pulse (area = 10 mm^2 real, so 90 μC real cm^{-2} pulse).

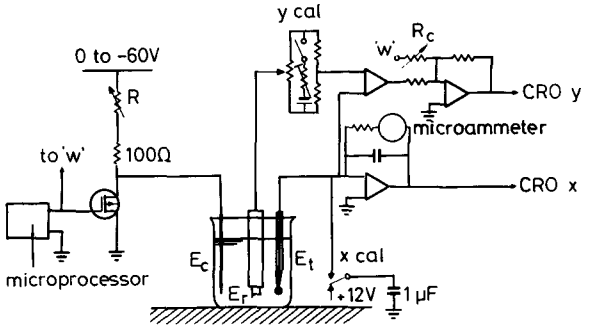

Fig. 10 *Further modification for studying a direct-coupled anode with optimal exhaustion*

2.7 *The direct-coupled pulsing cathode*

The apparatus shown in Fig. 7 is modified to pass current pulses through the electrode in the opposite direction; the power supply rail becomes positive and an *n*-channel FET replaces the *p*-channel. With t, T and R still equal to 20 ms, 60 ms and 30 kΩ, respectively, results are shown in Fig. 12, *a–g*, and are complementary to those in Fig. 8; there is a rapid fall in ϕ_1 from ϕ_0 to close to ϕ_{min} as charge per pulse is increased, limiting the safe injectible charge to about $-4\frac{1}{2}$ μC per pulse (Fig. 12*d*) (Area = 10 mm^2 real, so -45 μC real cm^{-2} pulse).

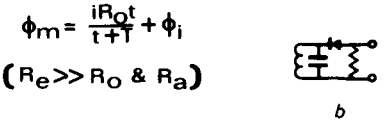

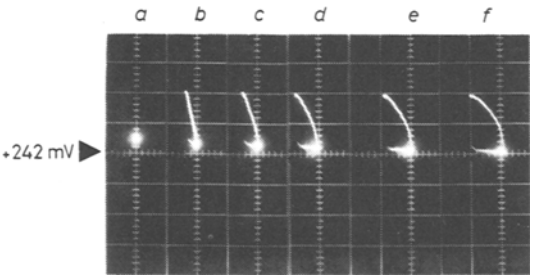

Fig. 11 *Family of ϕQ diagrams for a well exhausted direct-coupled anode. 20 ms pulse, 60 ms interval. Horizontal sensitivity: 9 μC division^{-1}, vertical sensitivity: 600 mV division^{-1}*

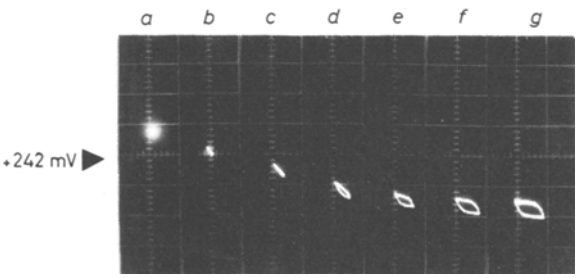

Fig. 12 *Family of ϕQ diagrams for a poorly exhausted direct-coupled cathode. Horizontal sensitivity: 9 μC division^{-1}, vertical sensitivity: 600 mV division^{-1}*

2.7.1 *The direct-coupled pulsing cathode with exhaustion.* A final modification of the ϕQ apparatus gives the opposite-current version of Fig. 10 (positive supply rail, *n*-channel FET). The results obtained with this are shown in Fig. 13, $a-f$; the change in horizontal scale should be noted. ϕ_1 remains close to ϕ_0. The diagram reaches Brummer's point between *d* and *e* and the electrode is probably working safely up to *f*, when it is injecting $-40\,\mu$ C per pulse (area = 9 mm^2 real, so $-360\,\mu$C real cm^{-2} pulse).

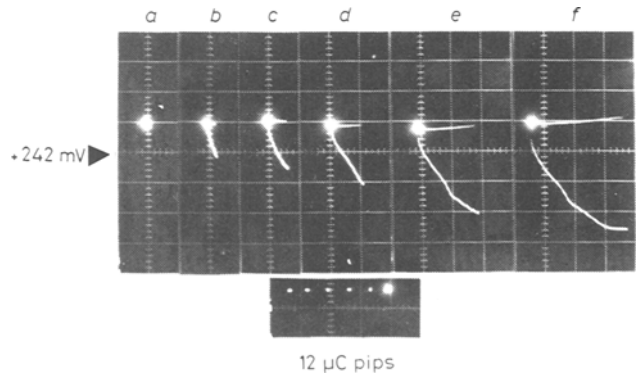

Fig. 13 *Family of ϕQ diagrams for well exhausted direct-coupled cathode. Horizontal sensitivity: 18 μC division^{-1}, vertical sensitivity: 600 mV division^{-1}*

Alternatively, one may idealise the diagram to two straight-line segments: the first, from ϕ_0 to Brummer's point, representing an oxide pseudocapacitance C_{e0} of 20 μF, or 180 μF real cm^{-2}; the second, from Brummer's point to ϕ_{min}, representing a hydride formation pseudocapacitance C_{eH} of 47 μF, or 420 μF real cm^{-2}. The injected charge per pulse *in vitro* is then

$$Q_C = -\int_{\phi_{min}}^{\phi_0} C_e\, d\phi$$

$$= -\int_{-400\,\mathrm{mV}}^{\phi_0} C_{e0}\, d\phi - \int_{\phi_{min}}^{-400\,\mathrm{mV}} C_{eH}\, d\phi$$

and putting +600 mV for ϕ_0,

$$Q_{c\,max} = -360\,\mu\mathrm{C\ real\ cm^{-2}}$$

The object of arriving by calculation at a figure which can be read straight off the diagram is to emphasise that the calculation also enables one to make a guess at what would happen *in vivo*. We saw in Section 2.1 that, in the monkey, $\phi_0 = +135$ mV. If this value is substituted, $Q_{c\,max} = -277\,\mu$C real cm^{-2}; likewise for a direct-coupled well exhausted anode *in vivo*

$$Q_{a\,max} = +\int_{\phi_0}^{\phi_{max}} C_{e0}\, d\phi$$

$$= +197\,\mu\mathrm{C\ real\ cm^{-2}}$$

2.7.2 *Efficiency of charge retrieval.* It is worth noting the excellent efficiency of charge retrieval from a well exhausted direct-coupled cathode. For example in Fig. 13*d*, injecting about half the maximum safe charge, namely 20 μC in 20 ms, the pulse current was evidently 1 mA. The average current supplied by the generator was therefore 250 μA. The net current read by the microammeter, which represents the net flux of charge lost through irreversible processes, was 0·6 μA. The efficiency of charge retrieval was therefore

$$\frac{250 - 0{\cdot}6}{250} \times 100 \text{ per cent} = 99{\cdot}76 \text{ per cent}$$

2.7.3 *The sliding of ϕ_1.* The slideback of ϕ_1 observed when a series capacitor is used may be regarded as beneficial, since it increases the potential range over which the electrode may be worked beyond what one would expect from considering ϕ_0 and the relevant limiting potential. Contrarily, the slide-forward observed with direct-coupled electrodes is always deleterious. It is therefore helpful to provide a series capacitor if room can be found for one. If room cannot be found, attention must be given to the stimulator circuitry, to obtain the best exhaustion possible. Note that the time constant for the decay of slide-forward is quite short (Fig. 9); it is approximately $C_e R_0$, say 20 μF and 5 kΩ, or 100 ms.

2.8 *Estimating safe limits of charge injection*

We have asserted, without supporting evidence, that the plateaus at top and bottom of the ϕQ diagram, at ϕ_{max} and ϕ_{min}, represent the onset of O_2 and H_2 evolution, respectively, and therefore the safe limits of charge injection. Two other possible criteria, applicable to any electrode, are colour changes in pH-sensitive indicators in the electrolyte and the first appearance of gas bubbles. The colour changes result from the local surplus of OH^- or H^+ ions which results from the discharge of H^+ to H_2 or OH^- to O_2, respectively. An additional criterion, applicable to direct-coupled electrodes, is the appearance of net direct current, measured by the meter in Fig. 7 and 10.

Looking at the limits, for the unexhausted anodal run portrayed in Fig. 8, suggested by (i) the appearance of bubbles, (ii) the position of the ϕ_{max} plateau and (iii) the net current, we see from Fig. 14*a* that a straight-line extrapolation of the net current back to zero cuts the axis at $4\frac{1}{2}$ μC per pulse, about the charge at which ϕQ flattening begins (Figs. 8*d* and *e*). However, the electrode appeared quiescent at this charge density, and no bubbling was seen until the charge per pulse reached 9 μC. Similarly, for the cathodal run portrayed in Fig. 12, the extrapolation back to zero occurs at 5 μC per pulse (Fig. 14*b*), which coincides well with the onset of flattening

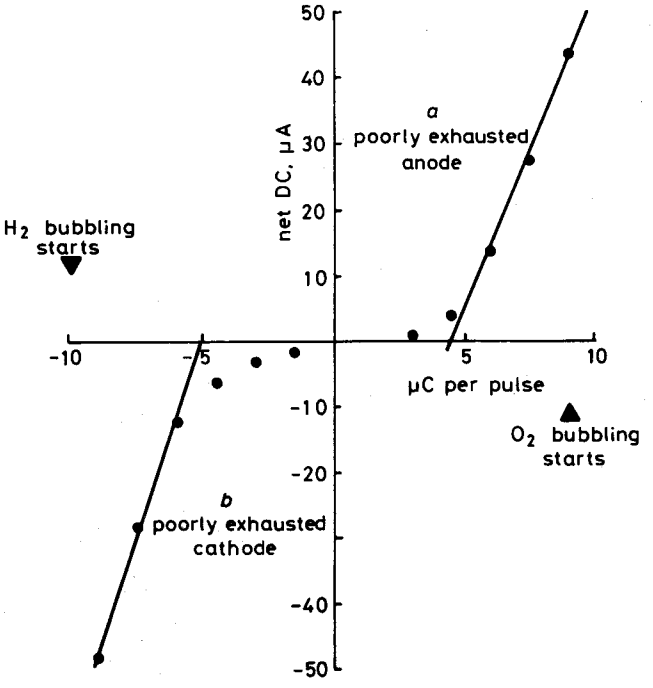

Fig. 14 *Relationship between net DC, bubbling and ϕQ flattening with direct-coupled electrodes; (a) anode, (b) cathode*

between Figs. 12*d* and *e*. Yet bubbling was not observed below 10 μC per pulse.

Evidently at the rather low current densities used in ϕQ studies, there is reasonable agreement between estimates of safe limits based on ϕQ flattening and on net current, but estimates derived from bubbling veer toward the optimistic. This is not really surprising. It is one thing to form monatomic H and O, quite another to assemble H_2 and O_2 molecules in sufficient numbers to form bubbles; discharged ions can be reconverted to H^+ and OH^- at the electrode, whereas gas molecules can diffuse away into solution. Even at the relatively high current density of 50 mA real cm^{-2}, Brummer and Turner estimated, for double pulses, an injectible charge, based on the onset of bubbling, of 400–420 μC real cm^{-2}, but a 'theoretical' non-gassing limit of only 300–350 μC real cm^{-2} (BRUMMER and TURNER, 1977*c*).

2.8.1 *Limitation of ϕQ studies.* The ϕQ diagram gives useful insight into the electrical behaviour of the platinum stimulating electrode, and into the electrochemical processes which underline that behaviour. To be conveniently interpretable, however, the potentials displayed must not be too far from the equilibrium potentials of the relevant reactions; i.e. the overpotentials should be low, which means current densities have also to be low ($\sim$0·1 A cm^{-2}). Pulse durations and pulse intervals have in consequence to be unrealistically long.

An electrode which has to deliver a full charge in 50 μs, say, will be operating at a current density approaching 10 A real cm^{-2}; the electrode dwell and plateau potentials will be obscured by the overpotentials and *IR* drops necessary to drive these large currents, and it becomes more profitable to turn to a new method of study which concentrates on electrode current and some way of estimating safe injectible charge which does not rely on potential measurement. We have seen that bubble-observation can be misleading; pH indicator methods, on the other hand, give good answers at high current densities, and require minimal apparatus. pH methods are considered in our companion paper (DONALDSON and DONALDSON, 1986).

3 Summary so far

We have traced the development of a notion that the 'safe' way to stimulate nervous tissue is to use active-balanced biphasic or 'Lilly' pulses. The truth of this idea may be unimportant in acute neurophysiological experiments, where the size and bulk of the stimulator is usually of little concern, and where the duration of stimulation is measured in hours. On the other hand, in neurological prostheses, stimulation may go on for years, but the stimulator needs to be as small and simple as possible. It becomes essential to decide whether formation of the relatively complex Lilly waveform is really necessary. We have measured the resting potential of a platinum electrode *in vivo*, and sought to show how resting potential affects the safe injectible charge. Finally, we have introduced the ϕQ diagram, which helps one to understand electrode behaviour for any repeating waveform, albeit up to moderate current densities only ($\sim$0·1 A cm^2). Our ϕQ studies show that, *in vitro*, capacitor-coupled electrodes delivering simple passive-balanced pulses, or direct-coupled well exhausted electrodes delivering passive-balanced cathodal pulses, can inject safely charge densities per pulse quite comparable to those for electrodes fed with Lilly waves.

References

BERKLEY, C. (1965) Potential problems in long term stimulation. Digest of the 6th International Conference on Medical and Biological Engineering, Tokyo.

BOCKRIS, J. O'M. and REDDY, A. K. N. (1970) *Modern electrochemistry*. Plenum Press, New York.

BOWDEN, F. P. (1929) The amount of hydrogen and oxygen present on the surface of a metallic electrode. *Proc. R. Soc.*, **125A,** 446–462.

BRUMMER, S. B. and TURNER, M. J. (1977*a*) Electrochemical considerations for safe electrical stimulation of the nervous system with platinum electrodes. *IEEE Trans.*, **BME-24,** 59–62.

BRUMMER, S. B. and TURNER, M. J. (1977*b*) Electrical stimulation with Pt electrodes I. *Ibid.*, **BME-24,** 436–439.

BRUMMER, S. B. and TURNER, M. J. (1977*c*) Electrical stimulation with Pt electrodes II. *Ibid.*, **BME-24,** 440–443.

BRUMMER, S. B., MCHARDY, J. and TURNER, M. J. (1977) Electrical stimulation with Pt electrodes III. *Brain Behav. Evol.*, **14,** 10–22.

DE BOER, R. W. and VAN OOSTEROM, A. (1978) Electrical properties of platinum electrodes: impedance measurements and time-domain analysis. *Med. & Biol. Eng. & Comput.*, **16,** 1–10.

DONALDSON, N. DE N. and DONALDSON, P. E. K. (1986) When are actively balanced biphasic ('Lilly') stimulating pulses necessary in neurological prostheses? II pH changes; noxious products; electrode corrosion; discussion. *Ibid.*, **24,** 50–56.

GREATBATCH, W. (1973) Electrochemical criteria for selection of chronically implanted stimulatory electrodes. In *Chronically implanted cardiovascular instrumentation.* MCCUTCHEON, P. (Ed.), Academic Press, New York, Chap. 19.

HOARE, J. P. (1967) *Advances in electrochemistry and electrochemical engineering, vol. 6,* DELAHAY, P. (Ed.), Interscience, New York.

LILLY, J. C., AUSTIN, G. M. and CHAMBERS, W. W. (1952) Threshold movements produced by excitation of cerebral cortex and efferent fibres with some parametric regions of rectangular current pulses. *J. Neurophysiol.*, **15,** 319–341.

LILLY, J. C., HUGHES, J. R., ALVORD, E. C. and GALKIN, T. W. (1955) Brief non-injurious electric waveforms for stimulation of the brain. *Science*, **121,** 468–469.

LOEB, J. C., MCHARDY, J., KELLIHER, E. M. and BRUMMER, S. B. (1982) Neural prostheses. In *Biocompatibility in clinical practice, Vol. II.* WILLIAMS, D. F. (Ed.), CRC Press. Chap. 8.

MCHARDY, J., ROBBLEE, L. S., MARSTON, J. M. and BRUMMER, S. B. (1980) Electrical stimulation with Pt electrodes IV. *Biomaterials*, **1,** 129–134.

ONARAL, B. and SCHWAN, H. P. (1982) Linear and nonlinear properties of platinum electrode polarisation. Part 1: frequency dependence at very low frequencies. *Med. & Biol. Eng. & Comput.*, **20,** 299–306.

PETERS, D. G. and LINGANE, J. J. (1962) Anodic formation and chemical analysis of oxychloride films on platinum electrodes. *J. Electroanal. Chem.*, **4,** 193–217.

ROBBLEE, L. S., MCHARDY, J., MARSTON, J. M. and BRUMMER, S. B. (1980) Electrical stimulation with Pt electrodes B. *Biomaterials*, **1,** 135–139.

ROBBLEE, L. S., LEFKO, J. L. and BRUMMER, S. B. (1983) Activated Ir: An electrode suitable for reversible charge injection in saline solution. *J. Electrochem. Soc.*, **130,** 731–733.

WEINMAN, J. and MAHLER, J. (1964) An analysis of electrical properties of metal electrodes. *Med. Electron. Biol. Eng.*, **2,** 299–309.

Appendix

On the resting potential of platinum

Since the electrode potential is below that for oxygen evolution, the oxygen evolution reaction must run backwards:

$$O_2 + 4H^+ \rightarrow 2H_2O - 4e$$

Call this reaction C, the cathodal reaction, whose equilibrium potential is ϕ_c. Reaction C is a common feature of metal corrosion in the presence of oxygen.

Similarly, since the electrode potential is above that for hydrogen evolution, this reaction also will run backwards:

$$2H_2 \rightarrow 4H^+ + 4e$$

so that, overall, the platinum is catalysing the production of water from hydrogen and oxygen. Call the latter reaction A, the anodal reaction whose equilibrium potential is ϕ_a. Reaction A is the one one wishes to have proceed rapidly in the hydrogen/oxygen fuel cell.

If the surface area of the electrode is Q, let a fraction θQ be operating anodally and $(1-\theta)Q$ cathodally. Then using the high-overvoltage simplification to the Butler-Vollmer equation (BOCKRIS and REDDY, 1970) the cathodal current is

$$(1-\theta)Qi_{0c}\, e^{\phi_c - \phi/\lambda}$$

where i_{0c} is the exchange current density for reaction C, ϕ is the electrode potential and λ is a constant.

Similarly, the anodal current is

$$\theta Q i_{0a}\, e^{\phi - \phi_a/\lambda}$$

If the electrode passes no external current, the anodal and cathodal currents must be equal.

$$(1-\theta)Qi_{0c}\, e^{\phi_c/\lambda} e^{-\phi/\lambda} = \theta Q i_{0a}\, e^{\phi/\lambda} \varepsilon^{-\phi_a/\lambda}$$

Therefore

$$e^{2\phi/\lambda} = \frac{1-\theta}{\theta}\frac{i_{0c}}{i_{0a}}\, e^{\phi_c + \phi_a/\lambda} \qquad (1)$$

The exchange current densities are

$$i_{0c} = FK_c C_c e^{-\gamma\phi_c}$$

where F is the Faraday, k_c the rate constant for reaction C, C_c the oxygen concentration and Υ a constant. Similarly

$$i_{0a} = FK_a C_a e^{-\Upsilon\phi_a}$$

where K_a is the rate constant for reaction A and C_a is the concentration of hydrogen. Therefore

$$\frac{i_{0c}}{i_{0a}} = \frac{K_c}{K_a}\frac{C_c}{C_a}\, e^{\Upsilon(\phi_a - \phi_c)} \qquad (2)$$

Putting eqn. 2 in eqn. 1 and taking logs

$$\frac{2\phi}{\lambda} = \ln\frac{K_c}{K_a} + \ln\frac{C_c}{C_a} + \ln\frac{1-\theta}{\theta} + \Upsilon(\phi_a - \phi_c) + \frac{\phi_c + \phi_a}{\lambda}$$

Therefore

$$\phi = \frac{\lambda}{2}\left\{\ln\frac{K_c}{K_a} + \ln\frac{C_c}{C_a} + \ln\frac{1-\theta}{\theta} + \Upsilon(\phi_a - \phi_c)\right\} + \frac{\phi_c + \phi_a}{2}$$

One cannot evaluate the above expression because one does not know what θ is. One knows *a priori* that ϕ_c is +0·8 V and ϕ_a is −0·4 V at pH 7, and that both move up and down together at the rate of 59 mV pH unit^{-1}. Therefore the term in $(\phi_a - \phi_c)$ is a constant, and one can write

$$\phi = K + \frac{\lambda}{2}\left\{\ln\frac{C_c}{C_a} + \ln\frac{1-\theta}{\theta}\right\} + \frac{\phi_c + \phi_a}{2}$$

The expression predicts a rise in electrode potential for an increase in dissolved oxygen, a decline in electrode potential for an increase in dissolved hydrogen, and a dependence on pH at the rate of 59 mV pH unit^{-1}. This is what is observed.

Authors' biographies

Nick Donaldson read Part 1 in Engineering and Part 2 in the Electrical Engineering tripos at Trinity College, Cambridge. During 15 months training at the Hirst Research Centre, GEC he developed an integrated circuit. Since 1976 he has worked at the Medical Research Council Neurological Prostheses Unit, mostly on implantable stimulators for functional electrical stimulation.

P. E. K. Donaldson was born in 1927 and educated at the Royal Naval College, Dartmouth and Cambridge University. He served in the Royal Navy from 1941 to 1952 and was a Technical Officer at the Physiological Laboratory, Cambridge University between 1953 and 1967. He has been on the engineering staff of the Medical Research Council Neurological Prostheses Unit since 1968.